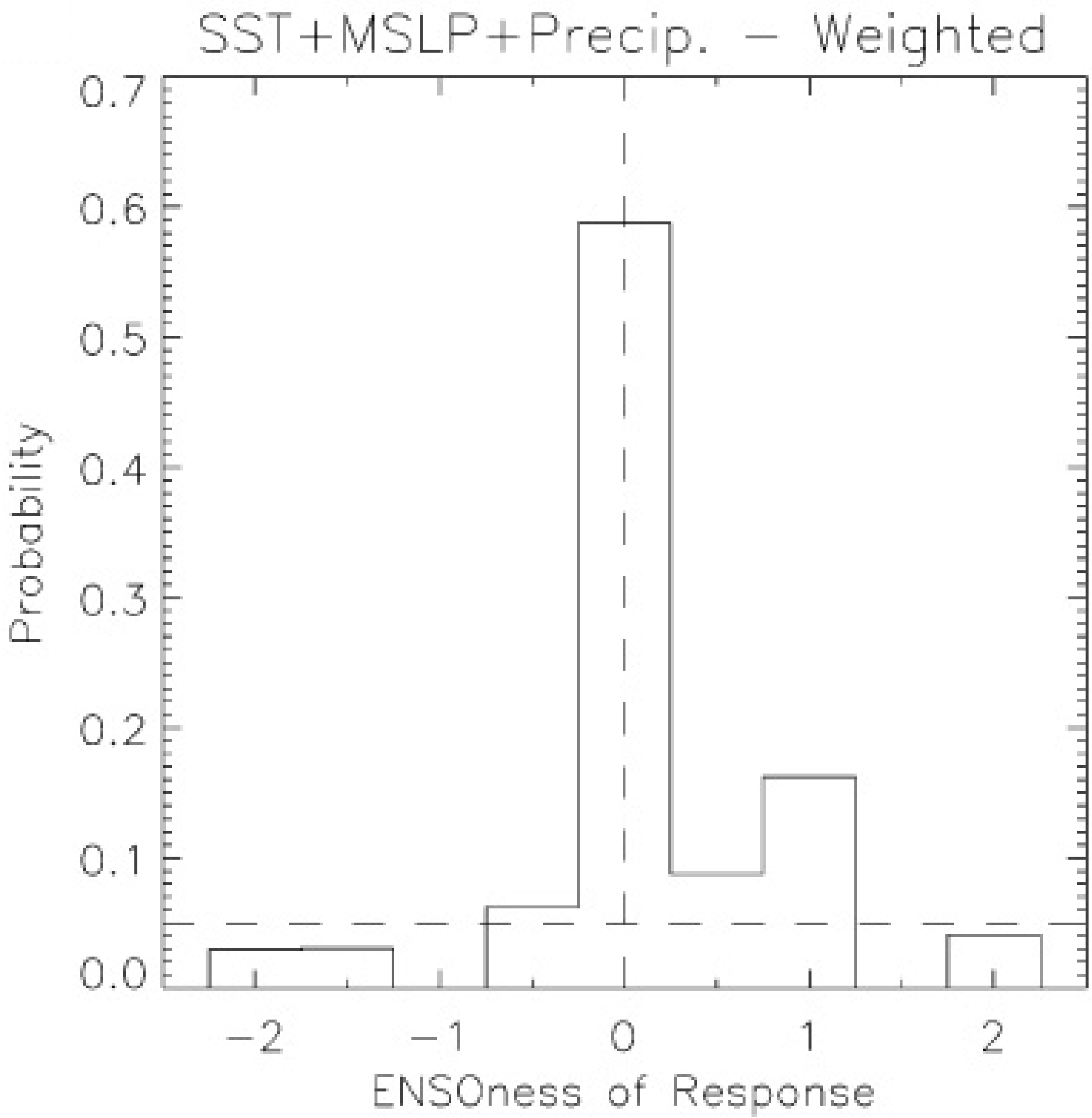

Figure 10.3.15. Weighted histograms of ENSOness of future mean trends in the tropical Pacific in the CMIP2 1%/year scenario. Positive ENSOness means El Niño-like mean state change. From Collins et al. (2005b).

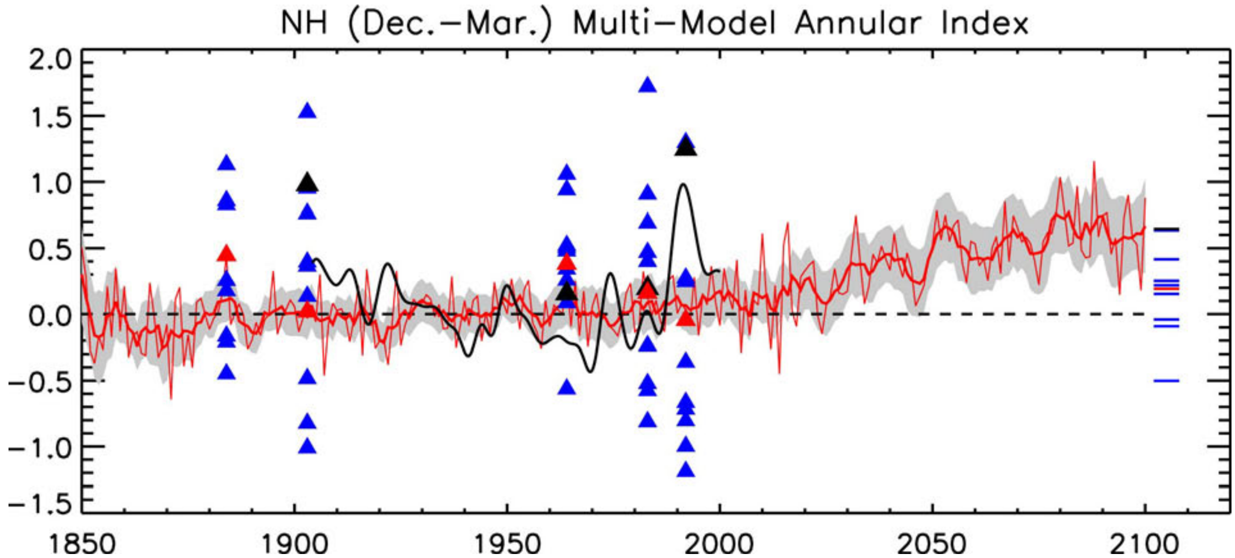

Figure 10.3.16. Multi-model average of the regression of the leading EOF of ensemble mean NH SLP with ensemble mean SLP (thin red). The time series of regression coefficients has zero mean between 1900 and 1970. The thick red line is a 5-year low-passed filtered version of the mean. The gray shading represents the inter-model spread at the 95% level and is filtered. A filtered version of the regression coefficient for Trenberth SLP is in black. The regression coefficient for the winter following a major tropical eruption is marked by red, blue, and black triangles, respectively, for the multi-model mean, the individual model mean, and observations. Bars at the far right indicate the multi-event composite response. From Miller et al. (2005).

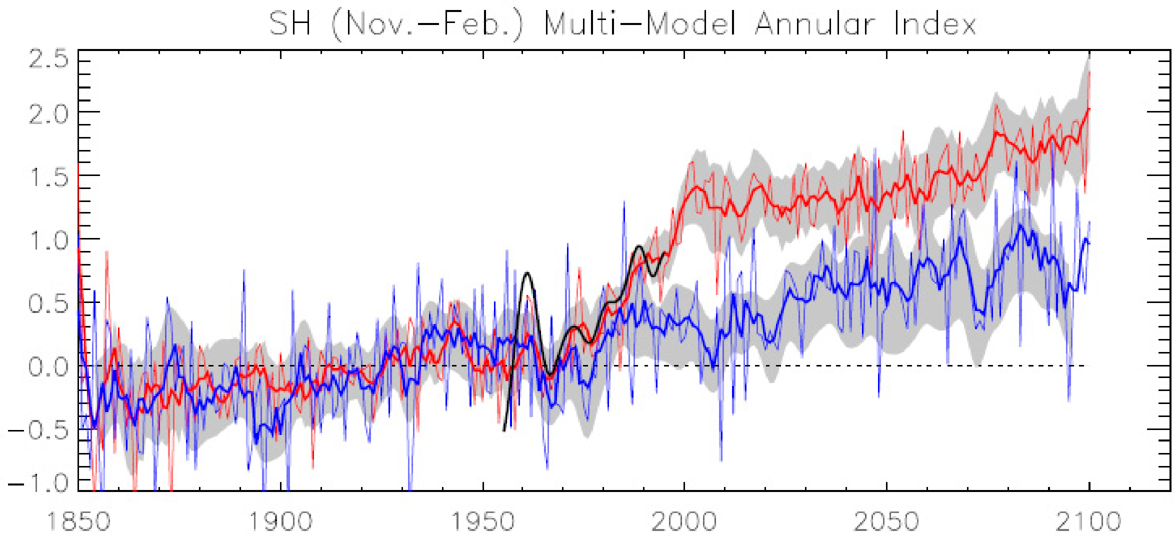

Figure 10.3.17. . Multi-model mean of the regression of the leading EOF of ensemble mean SH SLP with ensemble mean SLP for models with (red) and without (blue) ozone forcing. The time series of regression coefficients has zero mean between 1950 and 1999. The thick red and blue lines show a 5-year low-passed filtered version of the multi-model mean for models with and without ozone forcing, respectively. The gray shading represents the inter-model spread at the 95% level and is filtered. A filtered version of the regression coefficient for NCEP SLP is in black. From Miller et al. (2005).

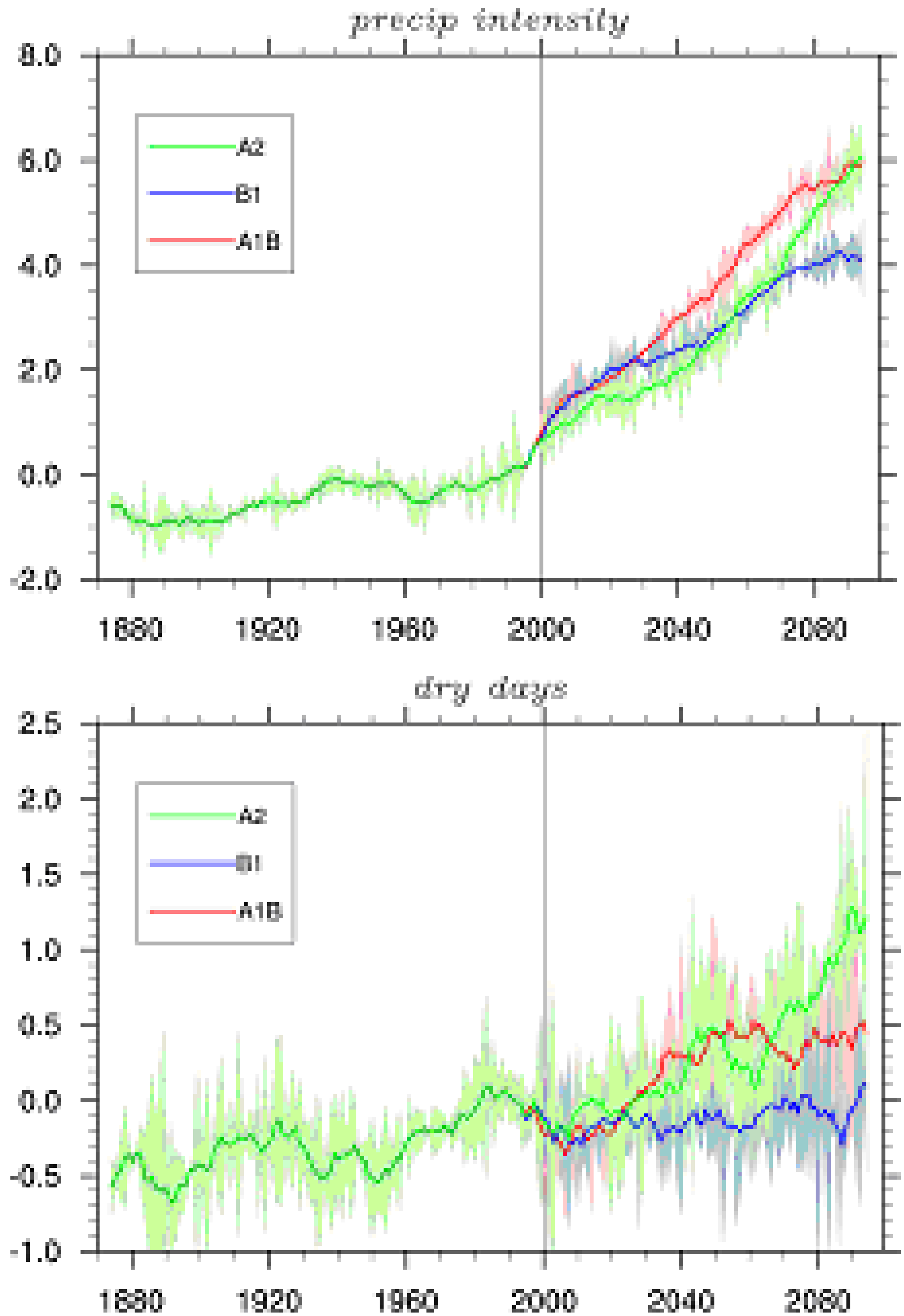

Figure 10.3.18. Globally averaged changes in precipitation intensity (top), and consecutive runs of dry days between precipitation events (below) computed from the Frich et al. (2002) extremes indices and compiled for eight global coupled climate models by Tebaldi et al. (2005). Solid line is the 10-year smoothed multi-model ensemble mean, The envelope of year-to-year variation before the 10-year smoothing is shown as background shading. Changes are given in units of standard deviations.

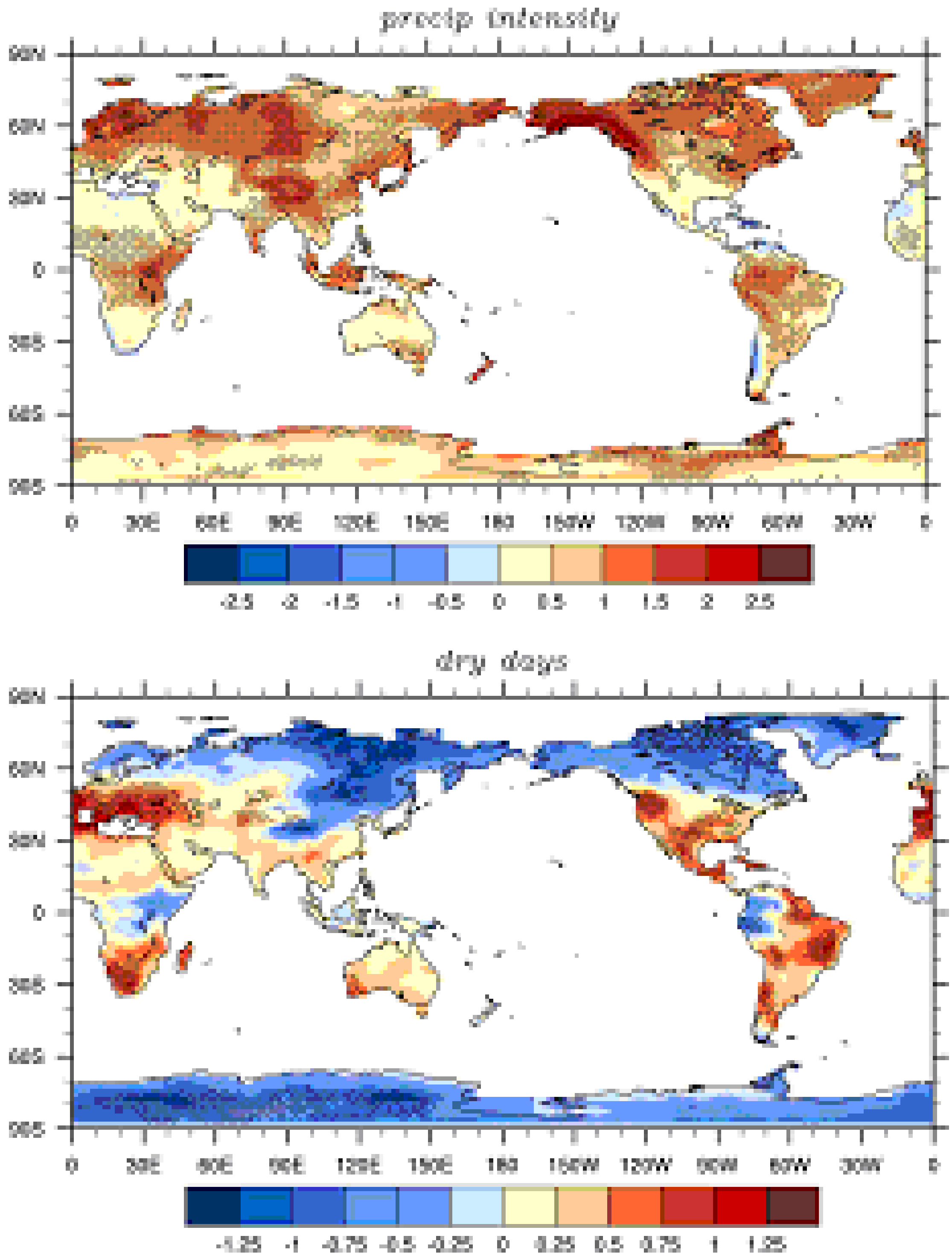

Figure 10.3.19. Changes in precipitation intensity (top), and consecutive runs of dry days between precipitation events (below) computed from the Frich et al. (2002) extremes indices and compiled for eight global coupled climate models by Tebaldi et al. (2005). Stippling indicates areas where at least four of the eight models show a statistically significant change. Changes are given in units of standard deviations.

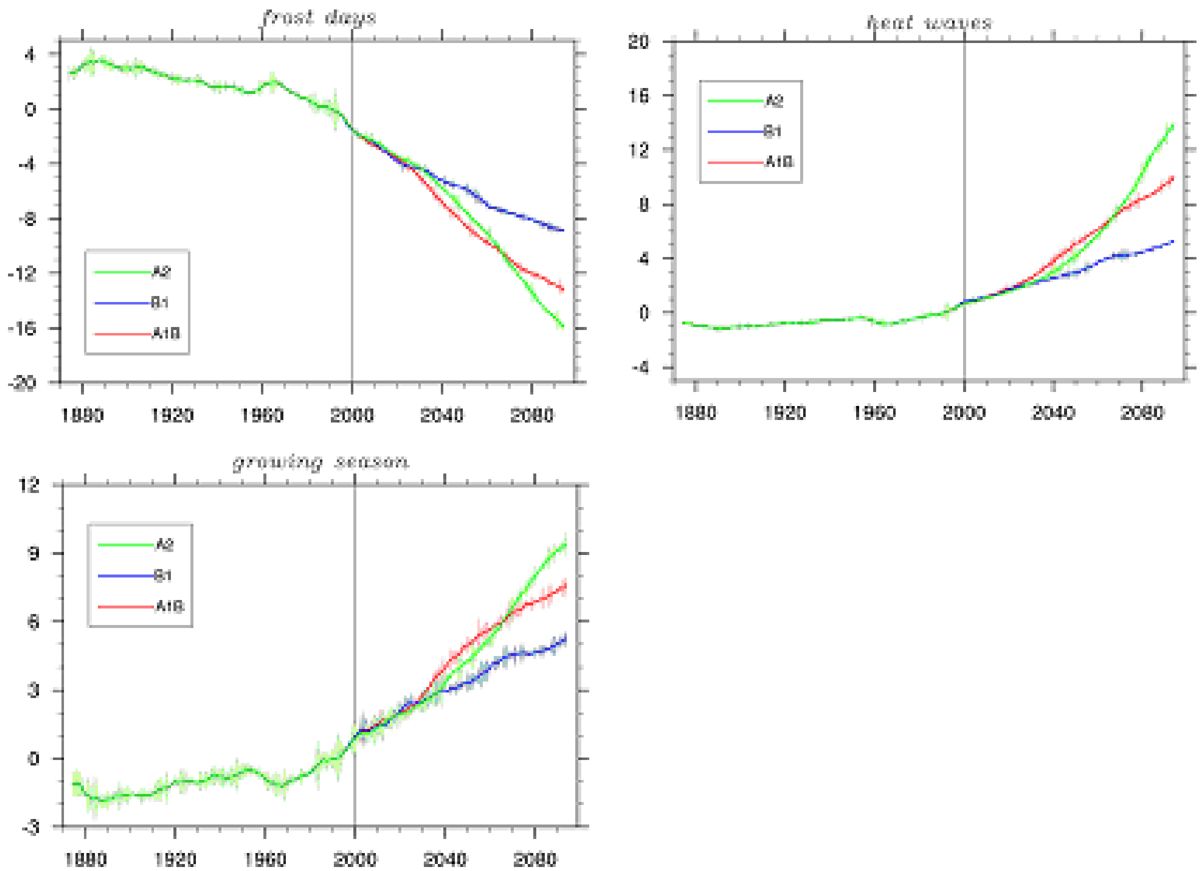

Figure 10.3.20. Globally averaged changes in frost days (upper left), heat waves (upper right), and growing season length (lower left) computed from the Frich et al. (2002) extremes indices and compiled for eight global coupled climate models by Tebaldi et al. (2005). Solid line is the 10-year smoothed multi-model ensemble mean, The envelope of year-to-year variation before the 10-year smoothing is shown as background shading. Changes are given in units of standard deviations.

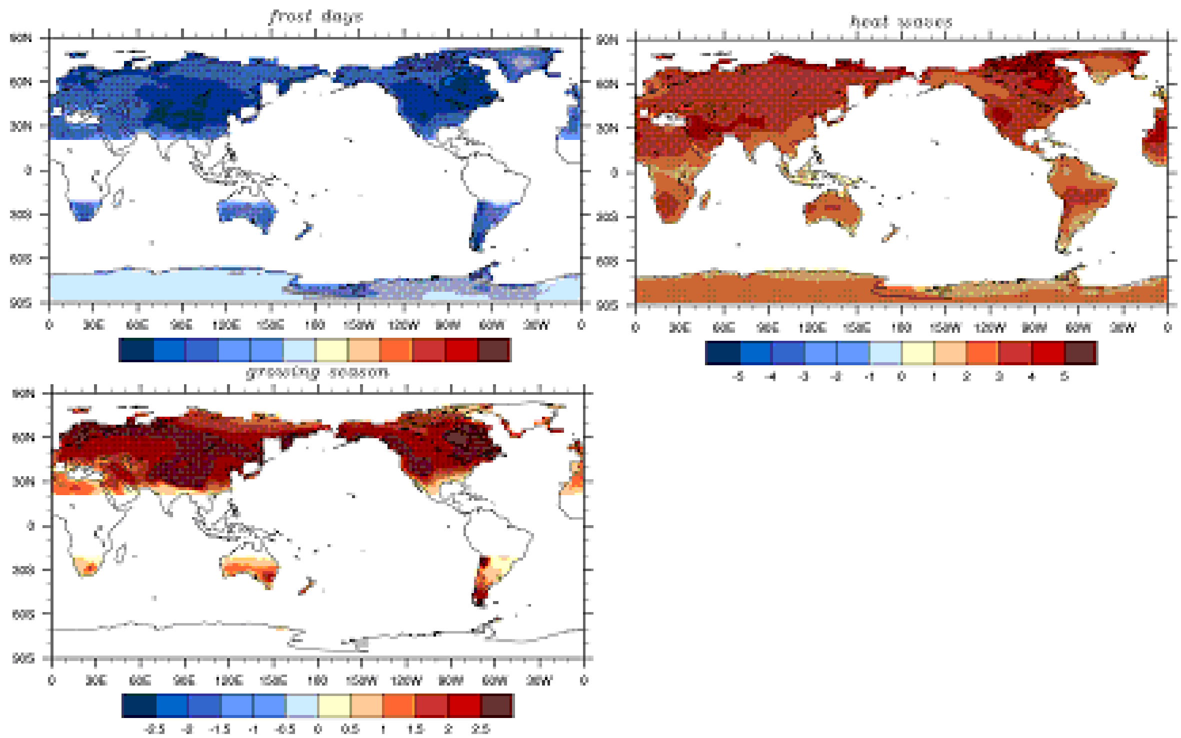

Figure 10.3.21. Changes in frost days (upper left), heat waves (upper right), and growing season length (lower left) computed from the Frich et al. (2002) extremes indices and compiled for eight global coupled climate models by Tebaldi et al. (2005). Frost days and growing season length are only for the extratropics. Stippling indicates areas where at least four of the eight models show a statistically significant change. Changes are given in units of standard deviations.

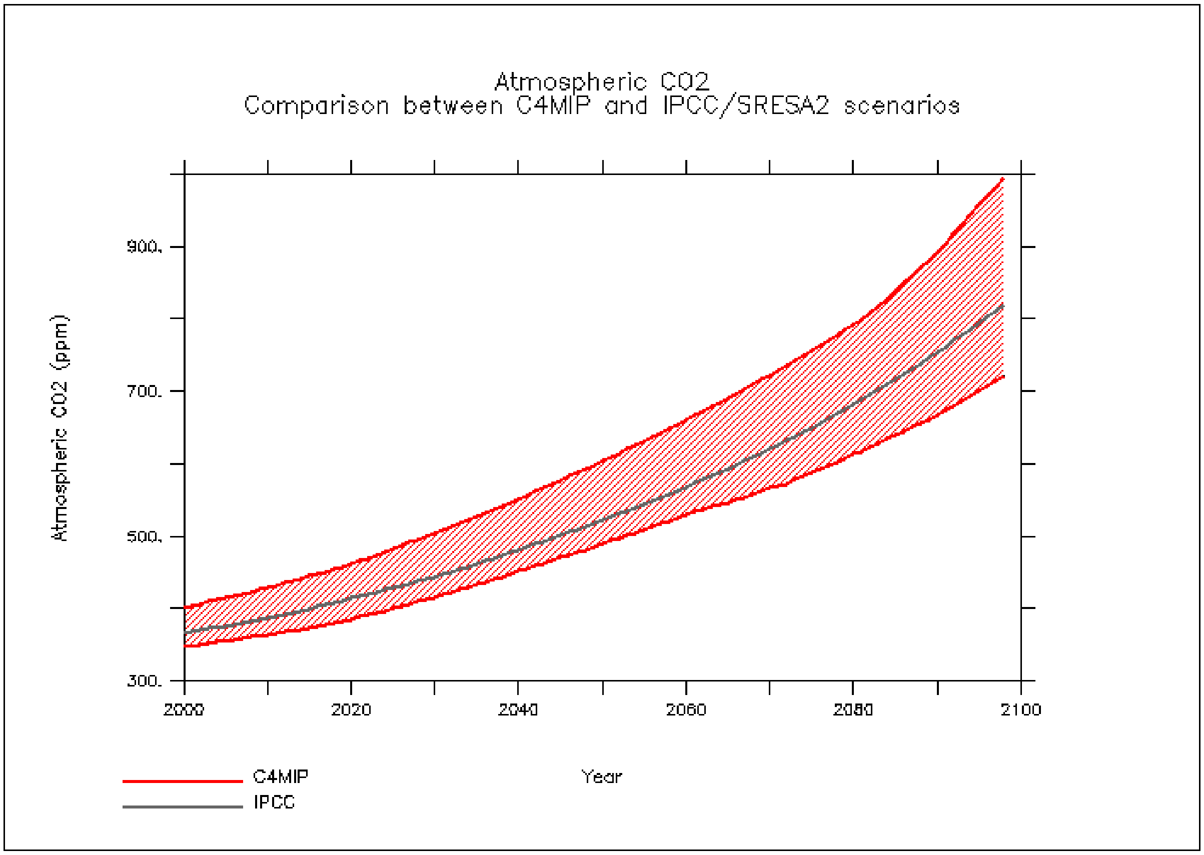

Figure 10.4.1. Envelope of the atmospheric CO_2 concentration simulated by the climate-carbon cycle coupled models (C4MIP) when driven by the SRES-A2 CO_2 emission scenario. Also shown in black is the atmospheric CO_2 concentration used by the standard climate models of the AR4 for the SRES-A2 scenario. That latter concentration was calculated beforehand by the BERN-CC model.

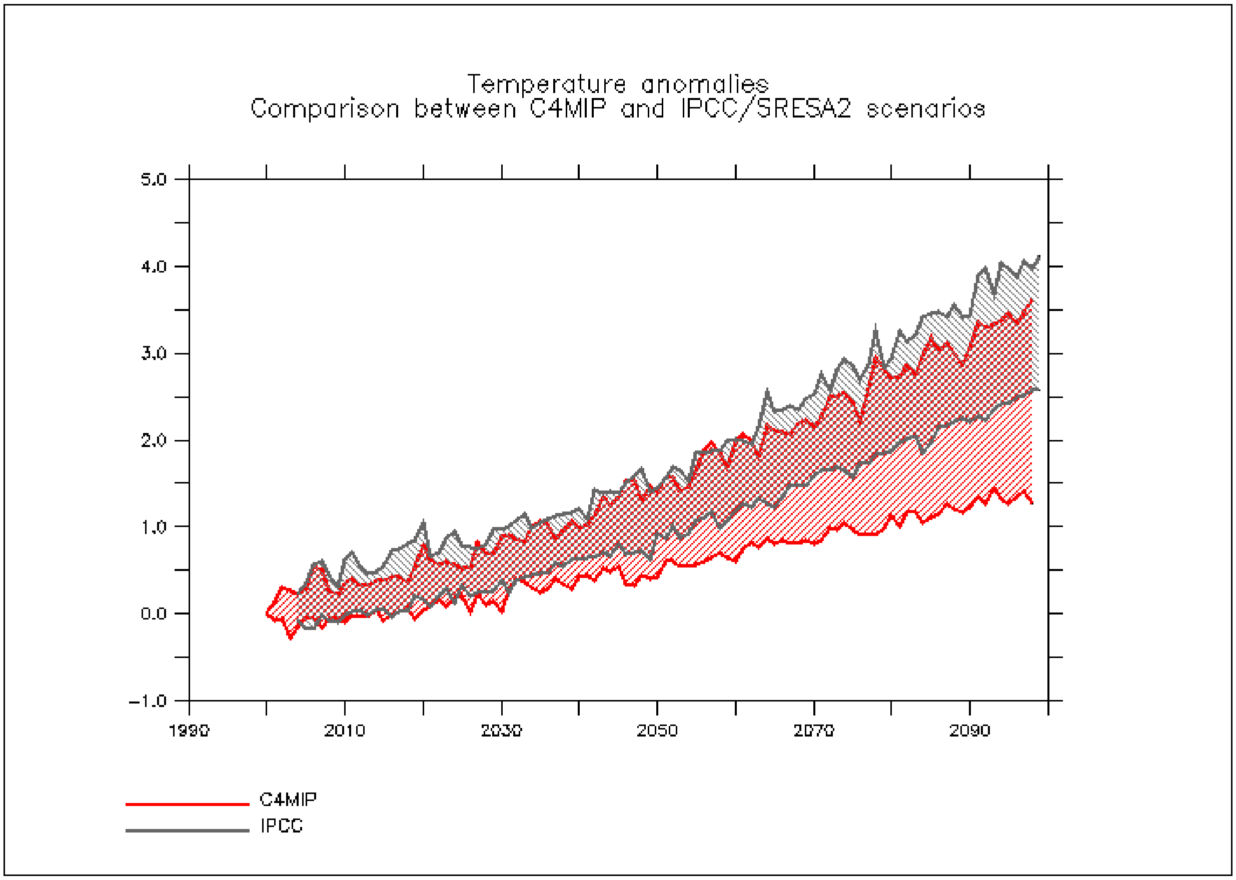

Figure 10.4.2. Envelopes of the global temperature change over the 21st century simulated by the C4MIP models (in red), and by the IPCC-AR4 climate models for the SRES-A2 scenario (in grey)

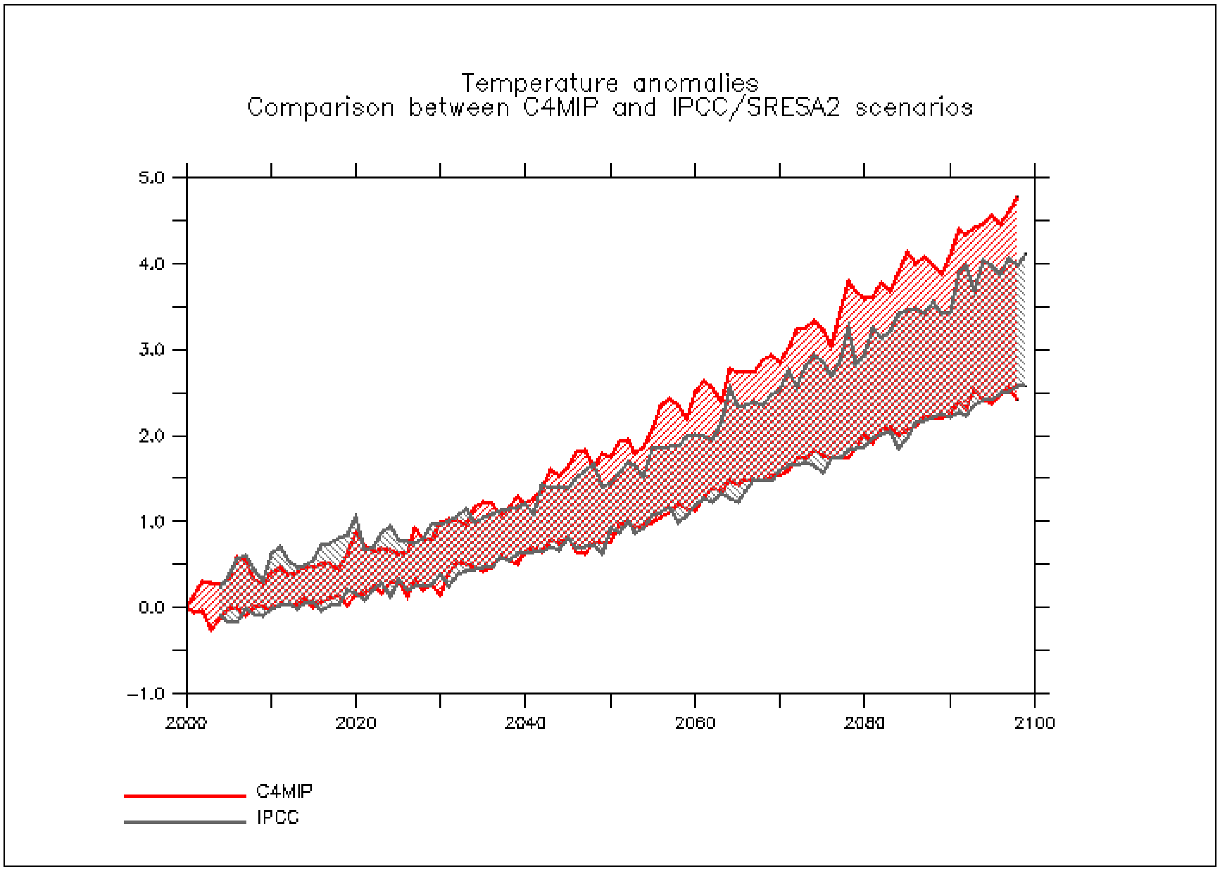

Figure 10.4.3. same as Figure 10.4.2, but with the C4MIP global temperature change corrected for the non-CO_2 greenhouse gases and aerosols radiative forcing.

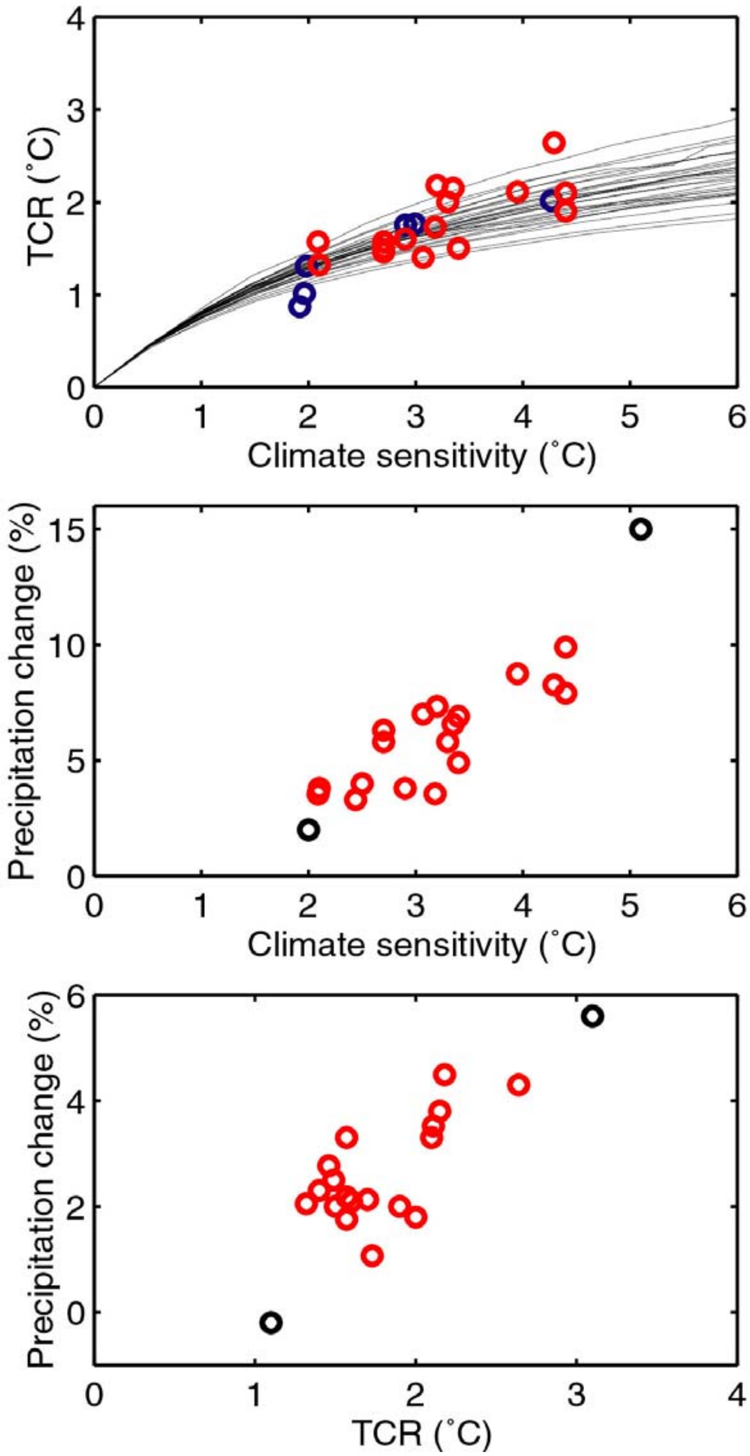

Figure 10.5.1. a) TCR versus climate sensitivity for all AOGCMs (red), EMICs (blue) and from a large ensemble of the Bern2.5D EMIC (Knutti et al., 2005) using different ocean vertical diffusivities and mixing parameterizations (black lines). b) Global mean precipitation change (%) as a function of global mean temperature change at equilibrium for doubling atmospheric CO_2 in slab ocean GCMs, c) Global mean precipitation change (in %) as a function of global mean temperature change (TCR) in a transient 1%/yr CO_2 increase scenario at the time of doubling, simulated by coupled AOGCMs.,

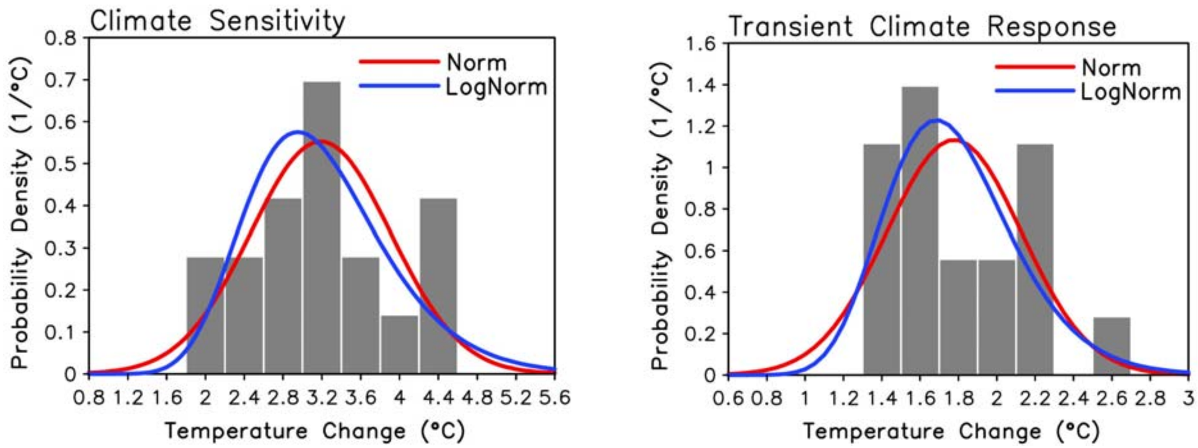

Figure 10.5.2. a) PDF fit to equilibrium climate sensitivity of the AR4 global coupled climate models, giving the normal and log-normal fits; b) same as top except for TCR. From Räisänen (2005c).

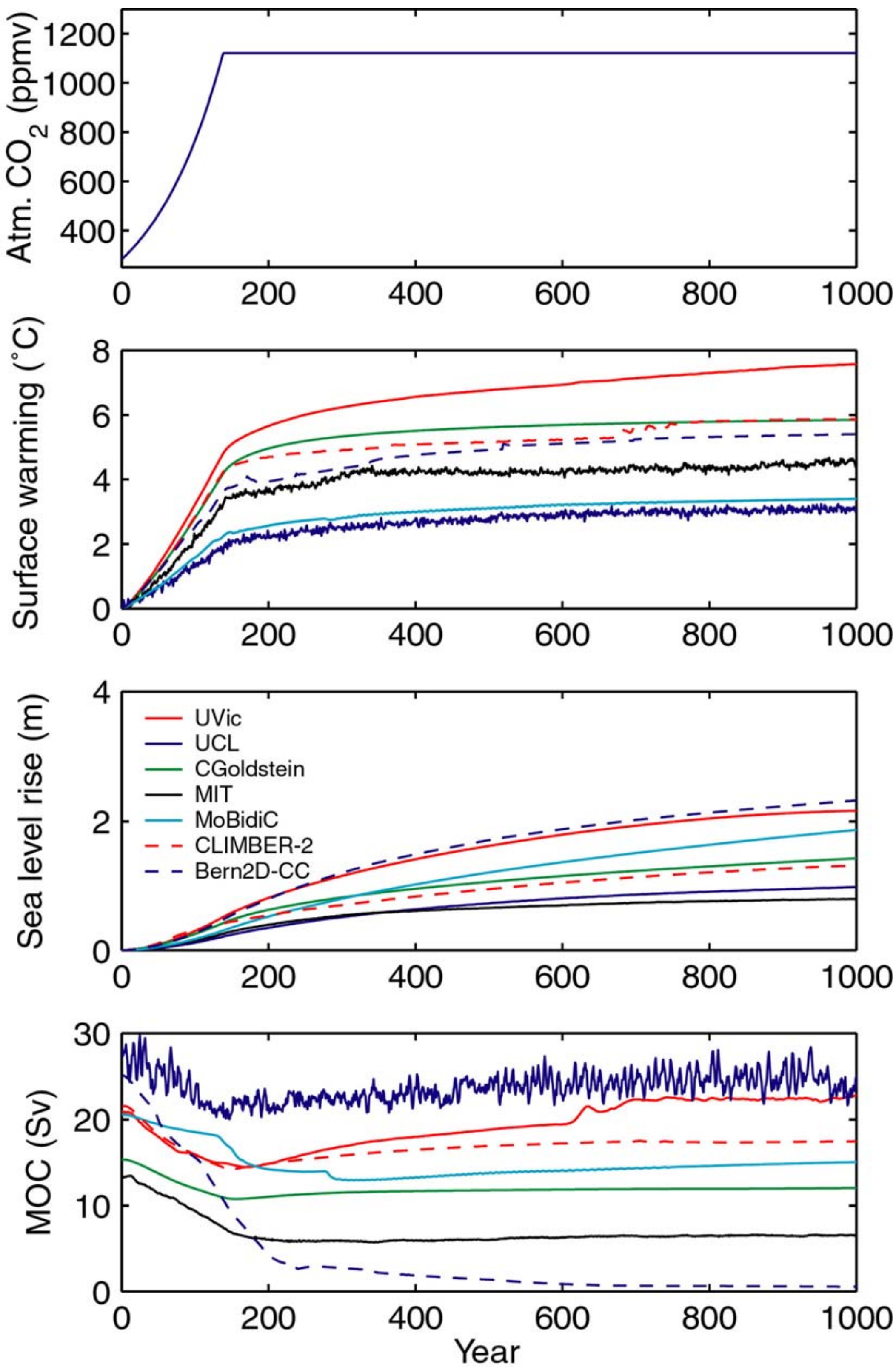

Figure 10.5.3. Surface warming, sea level rise from thermal expansion and meridional overturning (MOC) simulated by seven different EMICs for a fourfould increase of preindustrial CO_2 (1%/yr). The Bern model shows a shutdown of the MOC, resulting in an additional contribution to sea level rise.

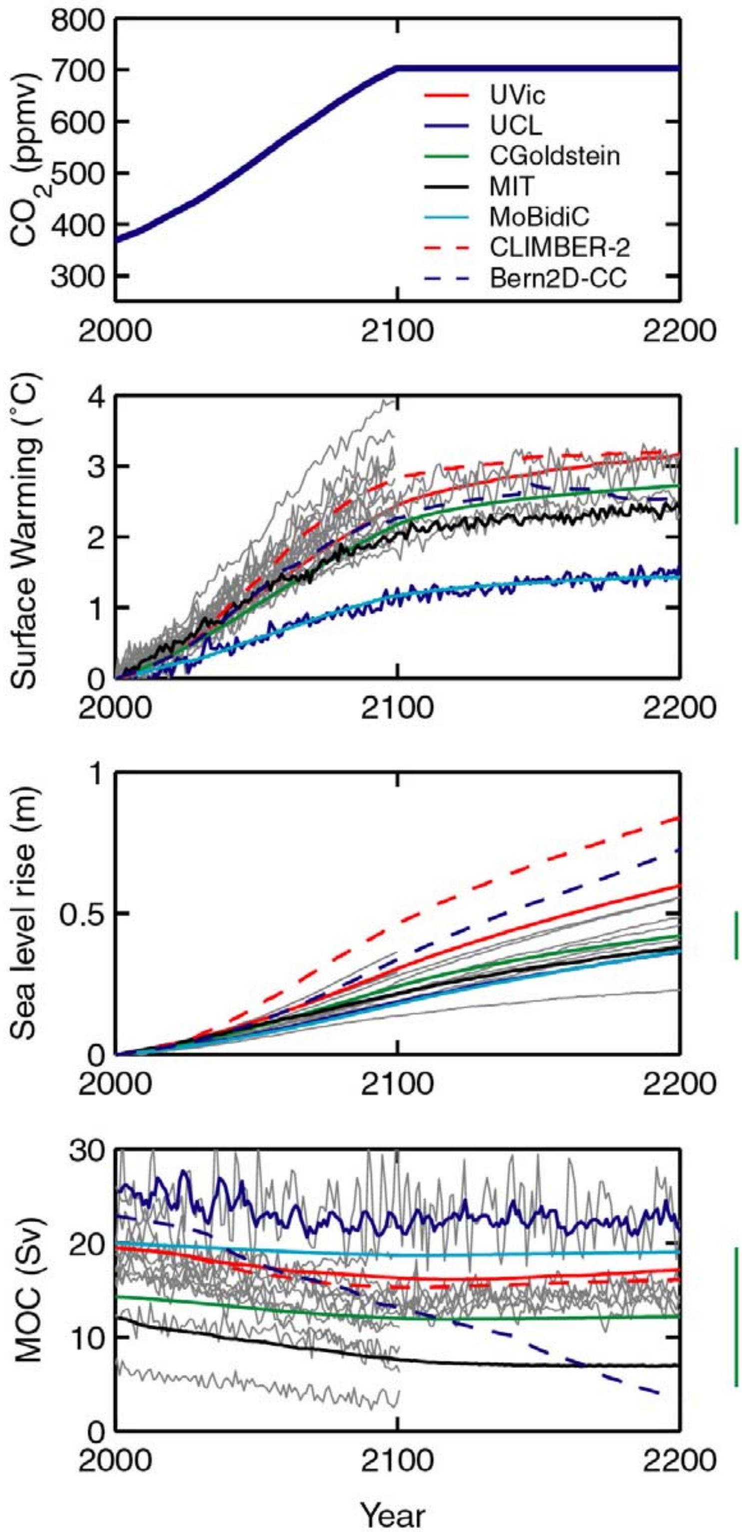

Figure 10.5.4. a) atmospheric CO_2, b) global mean surface warming, c) sea level rise from thermal expansion and d) Atlantic meridional overturning circulation for the SRES A1B scenario and stable radiative forcing after 2100. Coloured lines are results from seven intermediate complexity models, grey lines indicate AOGCM results where available for comparison. Vertical bars indicate plus/minus two standard deviation uncertainties due to ocean parameter perturbations in the Goldstein model.

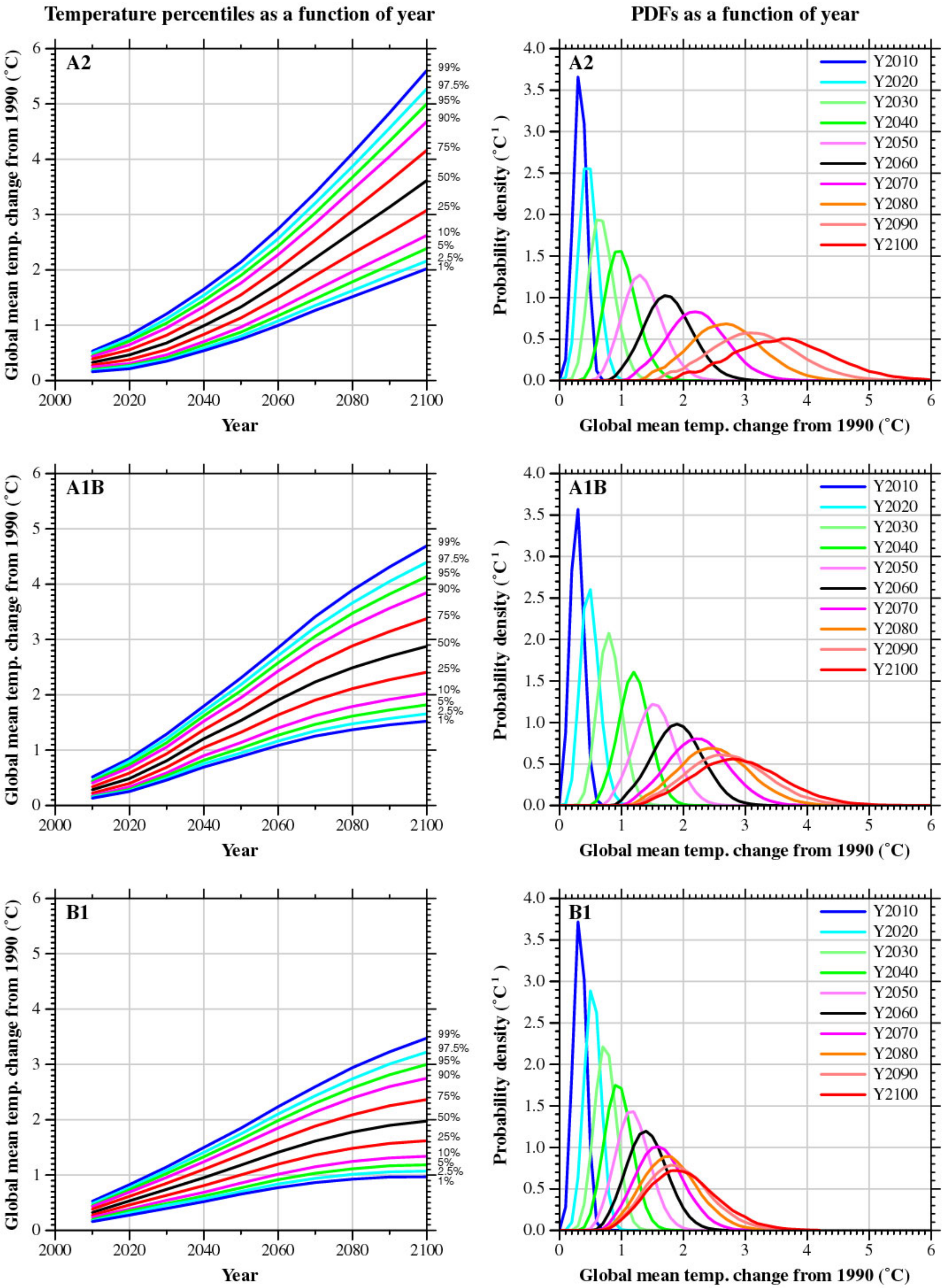

Figure 10.5.5. Simple climate model results for SRES scenarios A2, A1B and B1 from the analysis of Wigley and Raper (2001). Panels a, c, and e show temperature percentiles as a function of year. Panels b, d, and f show PDFs for temperature change relative to 1990.

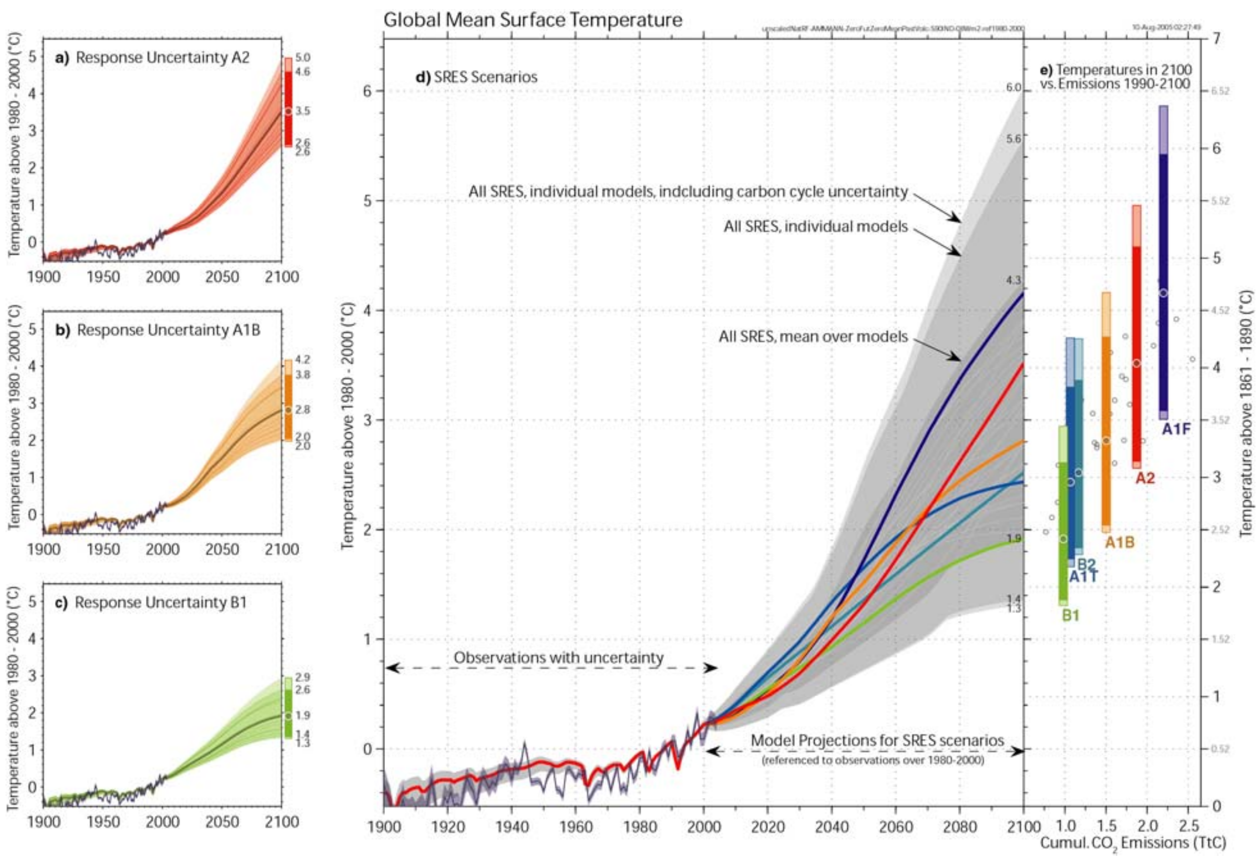

Figure 10.5.6. Observed global mean temperature change and future changes based on simple model results for the six illustrative SRES scenarios using a simple climate model tuned to eleven AOGCMs. The dark grey shading in panel d represents the envelope of the full set of thirty-five SRES scenarios using the simple model mean results over the eleven AOGCM tunings. The medium gray envelope represents the range of projections combining uncertainty in emissions (all 35 SRES scenarios) and models (all eleven AOGCM tunings). The light gray shading includes in addition uncertainties in the carbon cycle. The left side panels a to c depict response uncertainties for individual SRES scenarios A2, A1B and B1. The range of 2100 temperature projections for all 35 emission scenarios based on means over several models is plotted as circles in panel e) versus cumulative total (fossil and land use) CO_2 emissions on the bottom axis (1Terraton C = 1000 Gigatons C = 1000 Petagramm C). In addition, the “response uncertainties” for 2100 temperatures are given as bars for the six illustrative SRES scenarios with circles denoting the mean over models, dark uncertainty bands the range spanned by individual models and lighter shaded uncertainty bands the additional uncertainty due to different carbon cycle parameter choices.

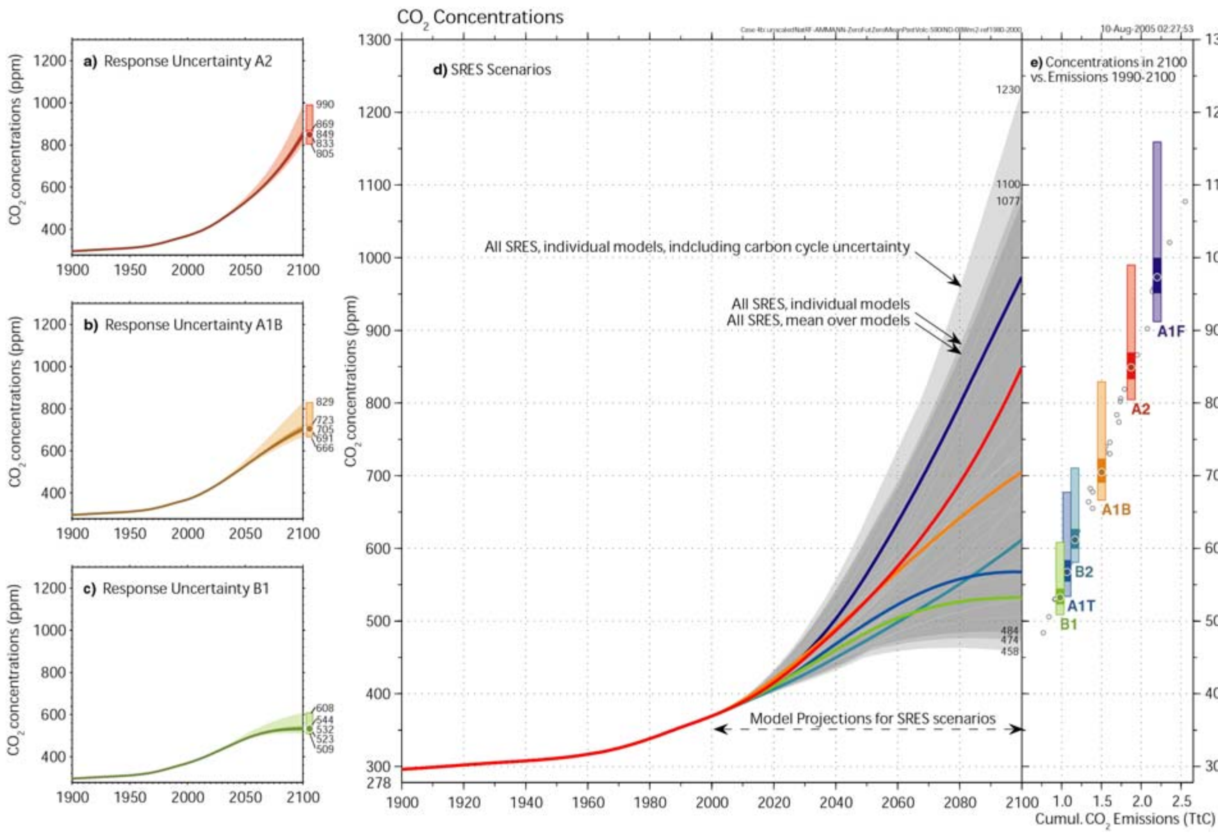

Figure 10.5.7. As Figure 10.5.6, but for CO_2 concentrations. Note that concentration uncertainties due to differences between models (dark colored bands in uncertainty bars in panel e) arise from different temperatures in each scenario combined with the default temperature feedback setting for the carbon cycle. Alternative temperature feedback settings that cover the range of uncertainty in complex carbon cycle models lead to the relatively large lighter shaded uncertainty bars (panel e).

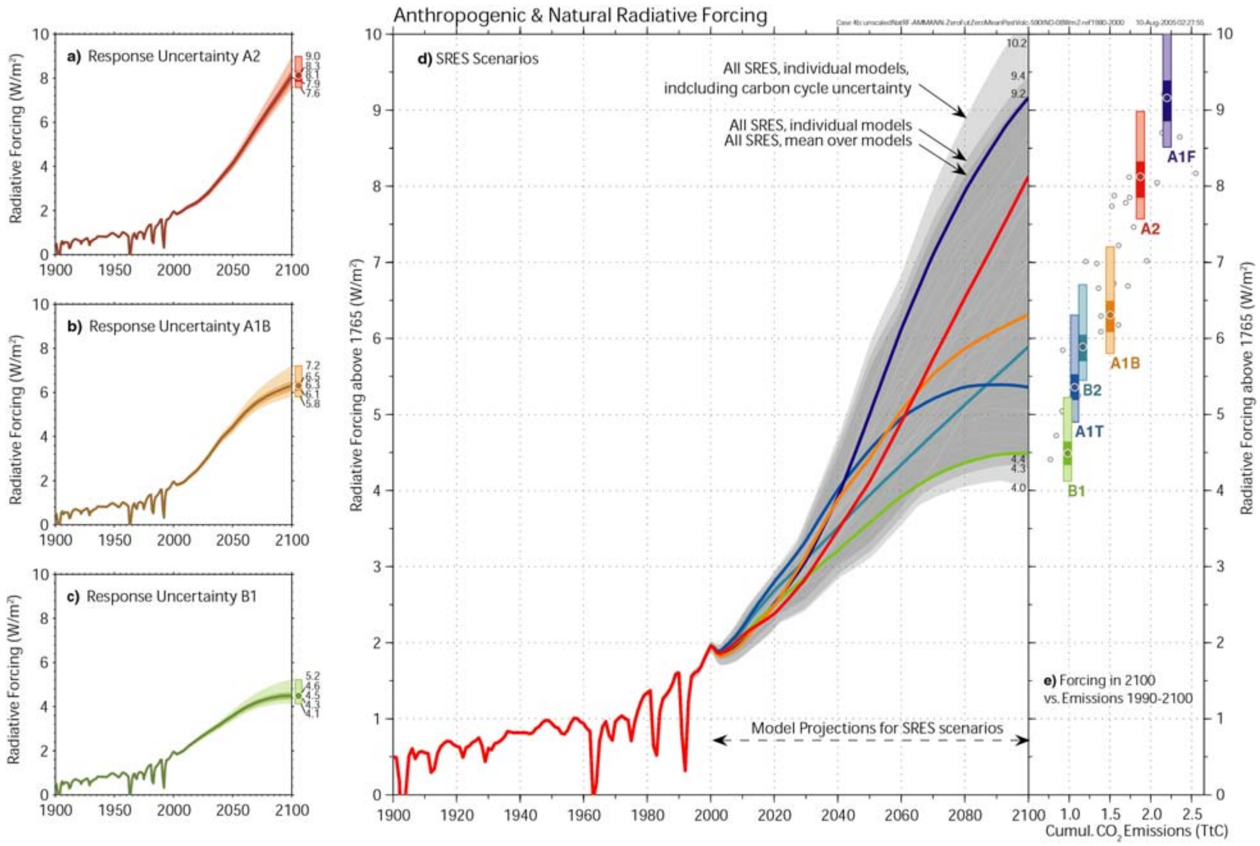

Figure 10.5.8. As Figure 10.5.6, but for total anthropogenic and natural forcing.

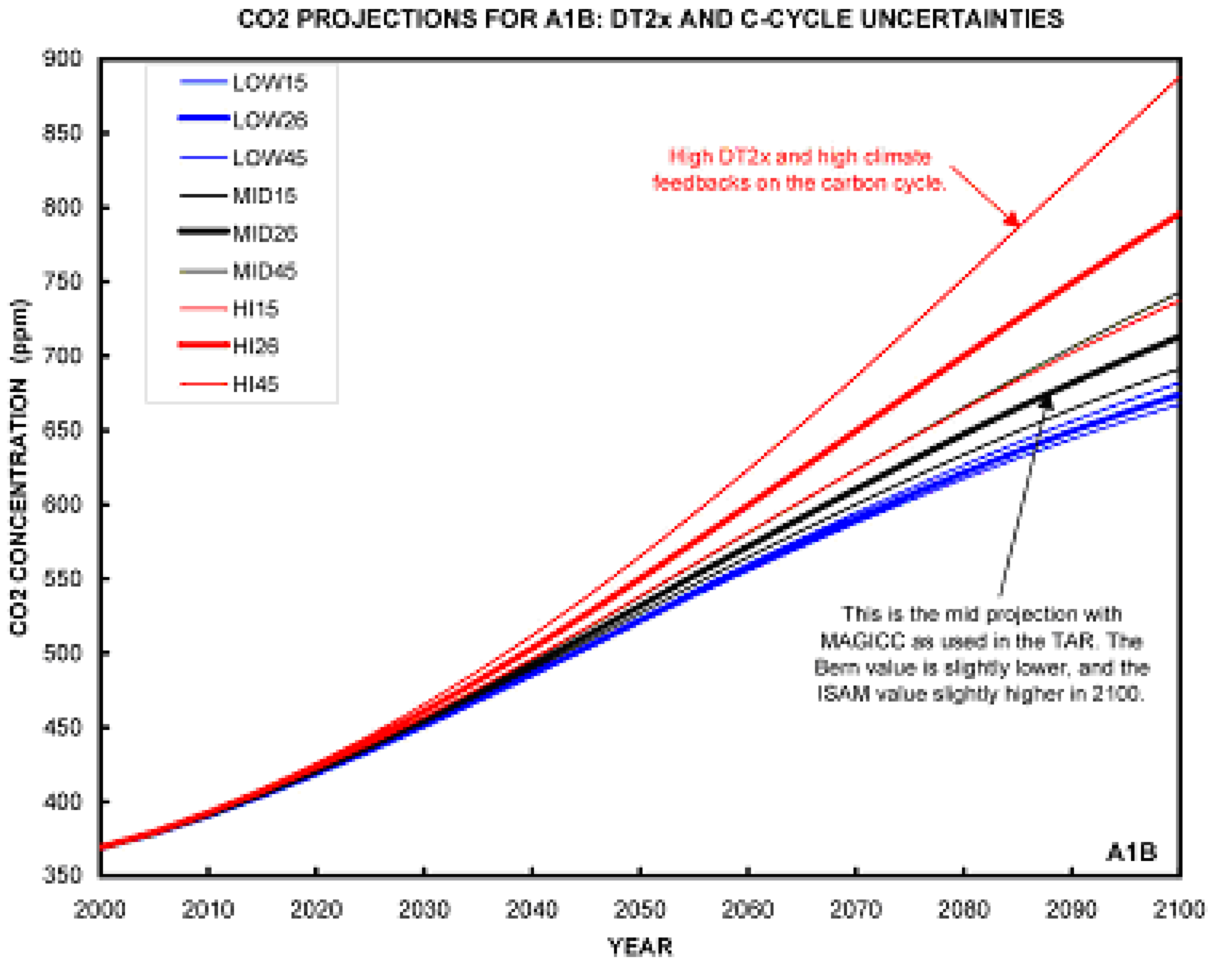

Figure 10.5.9. Simple model results illustrating CO_2 concentration uncertainties for scenario A1B associated with uncertainties in the carbon cycle.

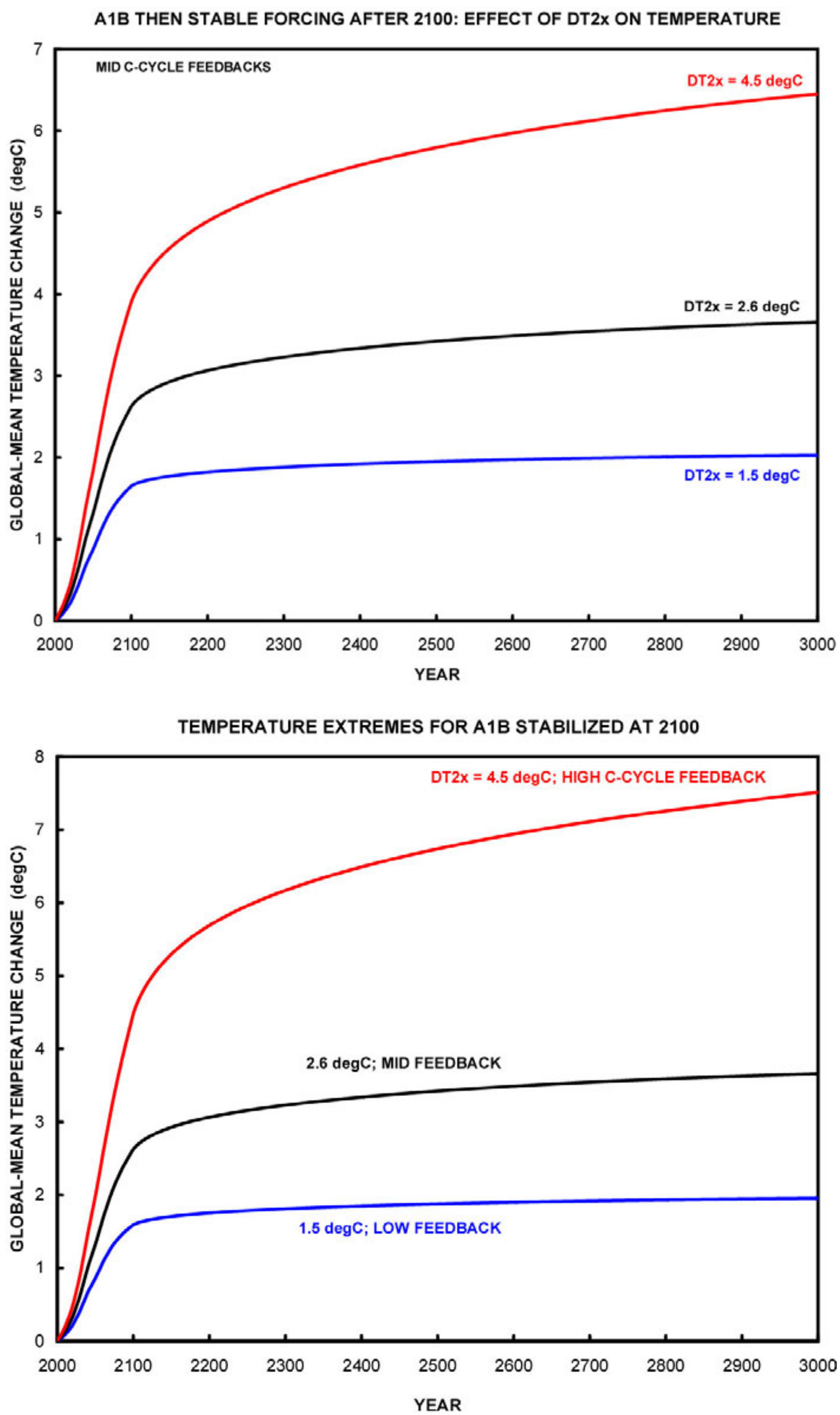

Figure 10.5.10. Simple climate model global mean temperature projections for a scenario that follows A1B CO_2 concentrations to 2100 followed by constant concentration (and, hence, radiative forcing). Panel a) shows the effect of climate sensitivity uncertainty, b) shows the ranges when carbon cycle uncertainties are considered.